Figure S1

A *Anti-Lamin A/C antibodies used in this study*

Lamin A/C Antibody	Antigen	Type	Catalog No.	Application (this study)
Anti-pS22	Synthetic phosphopeptide surrounding S22	Rabbit monoclonal	Cell Signaling D2B2E #13448	ELISA, ChIP, IF, Western of endogenous Lamin A/C
Anti-pan-N-terminal	Synthetic non-phospho peptide aa 2-29	Mouse monoclonal	Santa Cruz E1 sc-376248	ELISA, ChIP, IF, Western of endogenous Lamin A/C
Anti-full-length	Recombinant full length aa 1-664	Mouse monoclonal	Abcam 4C4 ab190380	ChIP, IF of transgene-derived WT & phospho-mutant Lamin A/C

B *Anti-pS22 specificity in ELISA*

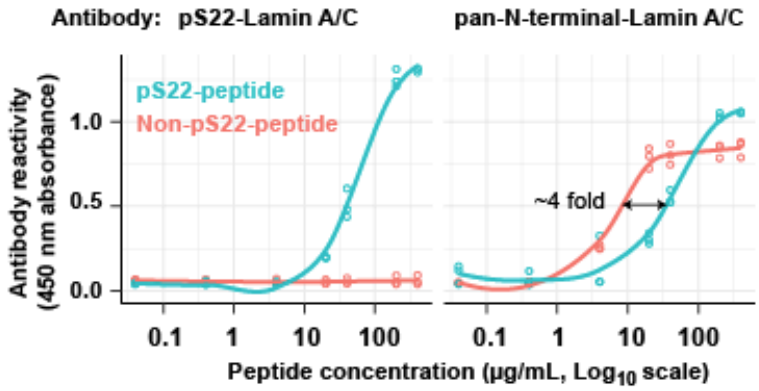

C *No antibody control for flow-cytometry*

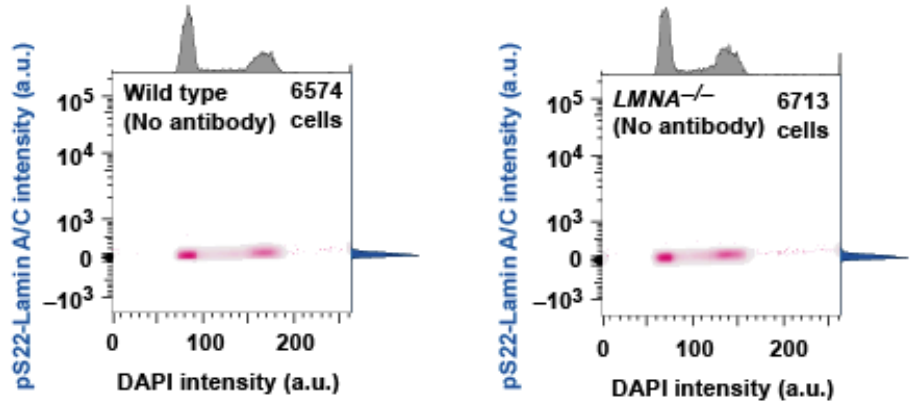

D *Entire Western blot shown in Fig. 1D*

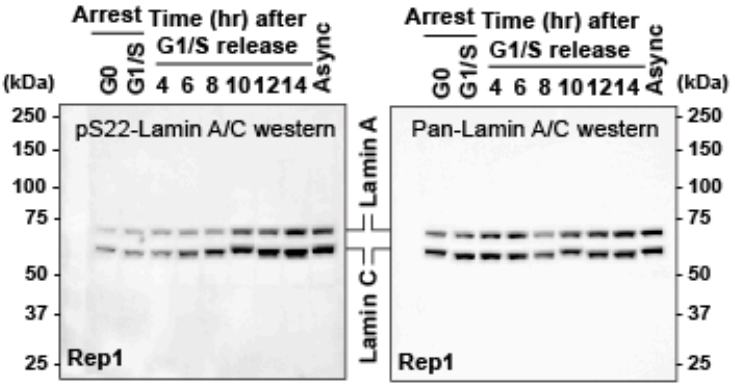

E *pS22-Lamin A/C western blot replicates*

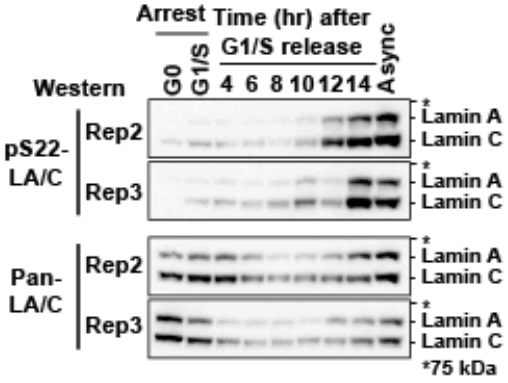

Figure S1. Characterization of S22-phosphorylated Lamin A/C (related to Figure 1)

(A) Anti-Lamin A/C antibodies used in this study.

(B) ELISA on immobilized synthetic phospho-S22 or non-phospho-S22-Lamin A/C peptides (aa2-29) incubated with anti-pS22-Lamin A/C or anti-pan-N-terminal-Lamin A/C antibodies. Circle, technical replicate. Line, Loess fit.

(C) Control flow cytometry analysis without anti-pS22-Lamin A/C antibody for **Fig. 1C**.

(D) Uncropped images of Western blots of synchronized wild-type BJ-5ta, part of which are shown in **Fig. 1D**. Left, blot detected with the anti-pS22-Lamin A/C antibody. Right, blot detected with the anti-pan-N-terminal-Lamin A/C antibody.

(E) (Top) Same as **D**, but two additional biological replicates are shown as cropped images.

Figure S2

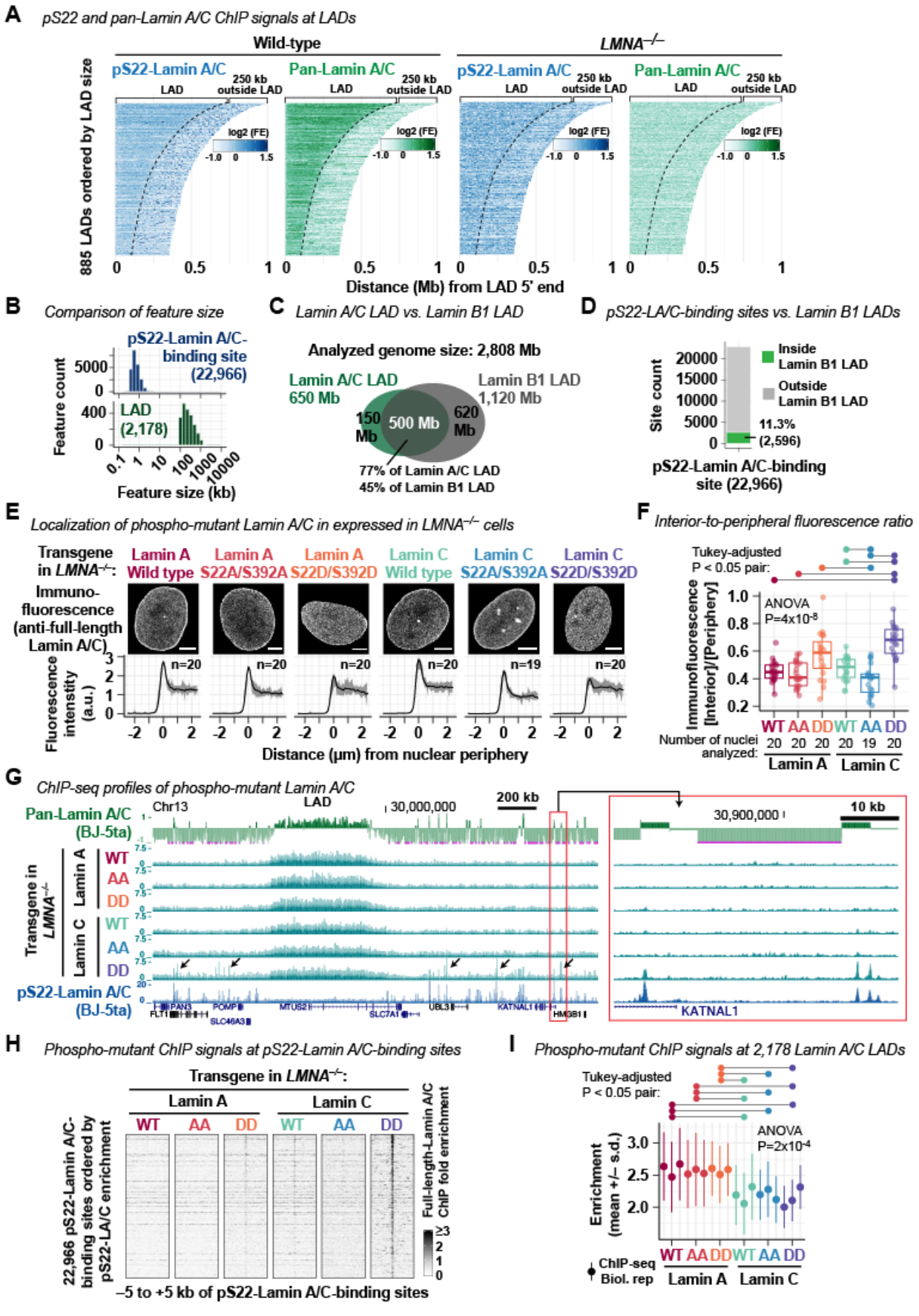
A
pS22 and pan-Lamin A/C ChIP signals at LADs
Wild-type
LMNA−/−
pS22-Lamin A/C
Pan-Lamin A/C
LAD
250 kb outside LAD
log2 (FE)
885 LADs ordered by LAD size
Distance (Mb) from LAD 5' end
B
Comparison of feature size
pS22-Lamin A/C-binding site (22,966)
LAD (2,178)
Feature count
Feature size (kb)
C
Lamin A/C LAD vs. Lamin B1 LAD
Analyzed genome size: 2,808 Mb
Lamin A/C LAD 650 Mb
Lamin B1 LAD 1,120 Mb
150 Mb
500 Mb
620 Mb
77% of Lamin A/C LAD
45% of Lamin B1 LAD
D
pS22-LA/C-binding sites vs. Lamin B1 LADs
Site count
Inside Lamin B1 LAD
Outside Lamin B1 LAD
11.3%
(2,596)
pS22-Lamin A/C-binding site (22,966)
E
Localization of phospho-mutant Lamin A/C in expressed in LMNA−/− cells
Transgene in LMNA−/−:
Lamin A Wild type
Lamin A S22A/S392A
Lamin A S22D/S392D
Lamin C Wild type
Lamin C S22A/S392A
Lamin C S22D/S392D
Immuno-fluorescence (anti-full-length Lamin A/C)
Fluorescence intenstity (a.u.)
n=20
n=19
Distance (μm) from nuclear periphery
F
Interior-to-peripheral fluorescence ratio
Tukey-adjusted P < 0.05 pair:
ANOVA P=4x10-8
Immunofluorescence [Interior]/[Periphery]
WT AA DD WT AA DD
Number of nuclei analyzed: 20 20 20 20 19 20
Lamin A
Lamin C
G
ChIP-seq profiles of phospho-mutant Lamin A/C
Chr13
LAD
30,000,000
200 kb
30,900,000
10 kb
Pan-Lamin A/C (BJ-5ta)
Transgene in LMNA−/−
Lamin A
Lamin C
WT
AA
DD
pS22-Lamin A/C (BJ-5ta)
KATNAL1
H
Phospho-mutant ChIP signals at pS22-Lamin A/C-binding sites
Transgene in LMNA−/−:
Lamin A
Lamin C
WT AA DD WT AA DD
22,966 pS22-Lamin A/C-binding sites ordered by pS22-LA/C enrichment
Full-length-Lamin A/C ChIP fold enrichment
≥3
–5 to +5 kb of pS22-Lamin A/C-binding sites
I
Phospho-mutant ChIP signals at 2,178 Lamin A/C LADs
Tukey-adjusted P < 0.05 pair:
ANOVA P=2x10-4
Enrichment (mean +/– s.d.)
WT AA DD WT AA DD
ChIP-seq Biol. rep
Lamin A
Lamin C

Figure S2. Characterization of pS22-Lamin A/C-binding sites (related to Figure 2)

(A) ChIP-seq fold-enrichment (FE) scores at Lamin A/C LADs defined by pan-N-terminal-Lamin A/C ChIP-seq. A subset of LADs that do not have adjacent LADs within 250 kb downstream of LADs are shown.

(B) Histogram of the size of pS22-Lamin A/C-binding sites and Lamin A/C LADs.

(C) Comparison of genomic domains covered by Lamin A/C LADs (in BJ-5ta, this study) or Lamin B1 LADs (lung fibroblast, Guelen et al., 2008).

(D) Location of pS22-Lamin A/C-binding sites with respect to the 1,302 Lamin B1 LADs.

(E) (Top) Immunofluorescence of transgene-driven Lamin A or Lamin C with phospho-deficient S22A/S392 mutations, or phospho-mimetic S22D/S392D mutations, or without mutation, expressed in *LMNA*$^{-/-}$ cells. The anti-full-length-Lamin A/C antibody (**Fig. S1A**) was used. (Bottom) Immunofluorescence signal distribution along a 5-μm segment that crosses the nuclear periphery at 0 μm (–2.5 to 2.5 μm with negative coordinates indicating positions outside the nucleus). Line, mean. Shade, minimum to maximum. n, number of nuclei analyzed.

(F) Interior-to-periphery Lamin A/C immunofluorescence signal ratio in transgene-driven wild-type (WT), phospho-deficient (AA), and phospho-mimetic (DD) Lamin A/C expressed in *LMNA*$^{-/-}$ cells. Interior signals are the mean signal within +4 to +5 μm of the aforementioned 5-μm segment. Peripheral signals are the maximum signal within -0.5 to +0.5 μm of the segment. One-way ANOVA compares the ratio of all isoforms, with post-hoc Tukey analysis for pairwise comparison (pairs with $P<0.05$ are indicated).

(G) Representative ChIP-seq profiles for transgene-driven wild-type (WT), phospho-deficient (AA), and phospho-mimetic (DD) Lamin A/C expressed in *LMNA*$^{-/-}$ cells. The anti-full-length-Lamin A/C antibody (**Fig. S1A**) was used in ChIP. Signals are FE scores. Pan-N-terminal Lamin A/C and pS22-Lamin A/C ChIP-seq profiles in BJ-5ta are shown for comparison. Arrows indicate positions at which phospho-mimetic Lamin C was enriched at pS22-Lamin A/C binding sites.

(H) ChIP-seq FE scores at the 22,966 pS22-Lamin A/C-binding sites.

(I) ChIP-seq FE scores across the 2,178 Lamin A/C LADs for each biological replicate. Mean of all FE scores within one LAD represents the FE score of that LAD. One-way ANOVA compares means of all isoforms, with post-hoc Tukey analysis for pairwise comparison (pairs with $P<0.05$ are indicated).

Figure S3

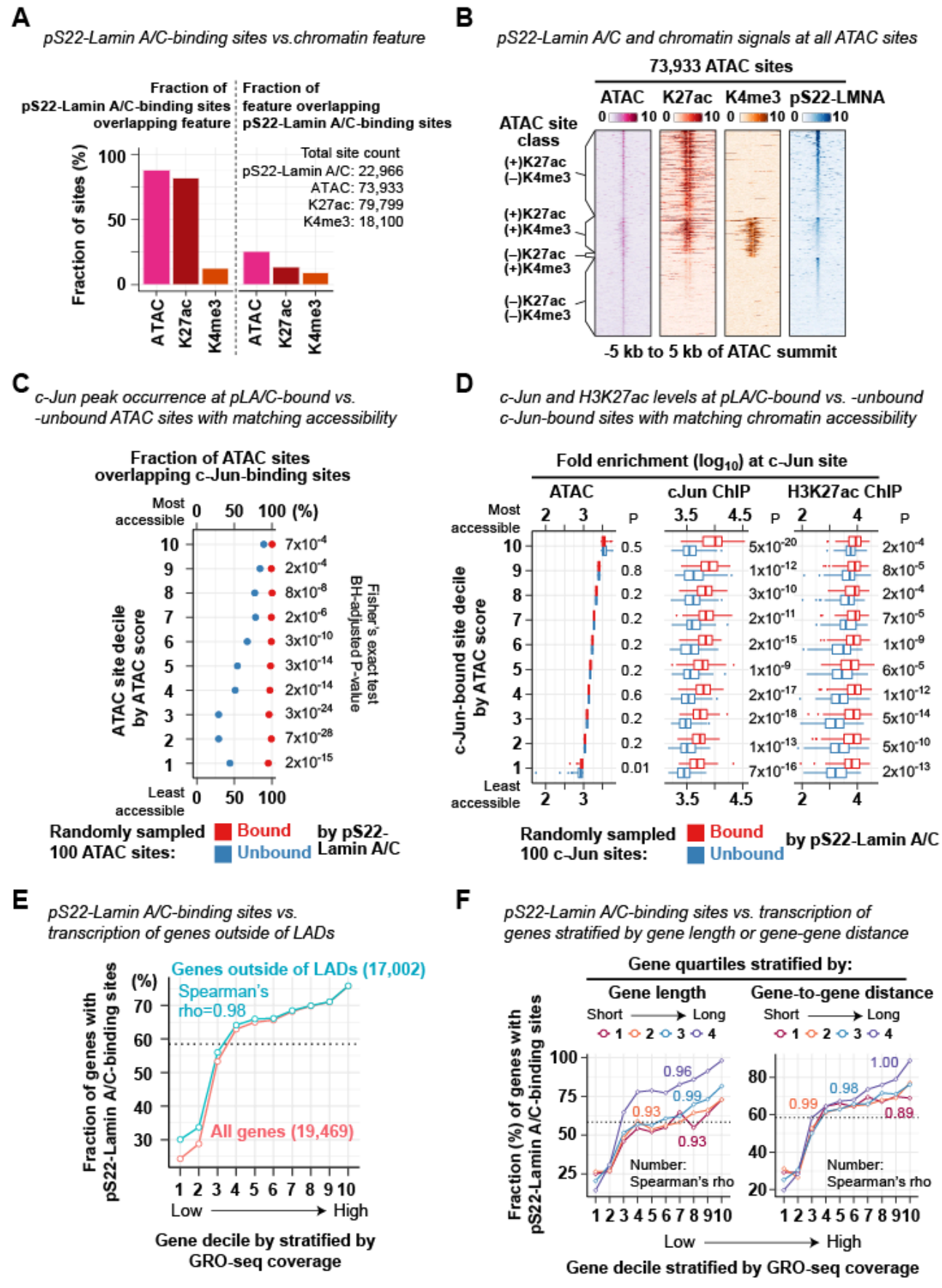
A
pS22-Lamin A/C-binding sites vs.chromatin feature
Fraction of pS22-Lamin A/C-binding sites overlapping feature
Fraction of feature overlapping pS22-Lamin A/C-binding sites
Fraction of sites (%)
Total site count
pS22-Lamin A/C: 22,966
ATAC: 73,933
K27ac: 79,799
K4me3: 18,100
ATAC
K27ac
K4me3
B
pS22-Lamin A/C and chromatin signals at all ATAC sites
73,933 ATAC sites
ATAC
K27ac
K4me3
pS22-LMNA
ATAC site class
(+)K27ac (–)K4me3
(+)K27ac (+)K4me3
(–)K27ac (+)K4me3
(–)K27ac (–)K4me3
-5 kb to 5 kb of ATAC summit
C
c-Jun peak occurrence at pLA/C-bound vs. -unbound ATAC sites with matching accessibility
Fraction of ATAC sites overlapping c-Jun-binding sites
Most accessible
Least accessible
ATAC site decile by ATAC score
Fisher's exact test BH-adjusted P-value
Randomly sampled 100 ATAC sites:
Bound
Unbound
by pS22-Lamin A/C
D
c-Jun and H3K27ac levels at pLA/C-bound vs. -unbound c-Jun-bound sites with matching chromatin accessibility
Fold enrichment (log10) at c-Jun site
ATAC
cJun ChIP
H3K27ac ChIP
c-Jun-bound site decile by ATAC score
Randomly sampled 100 c-Jun sites:
Bound
Unbound
by pS22-Lamin A/C
E
pS22-Lamin A/C-binding sites vs. transcription of genes outside of LADs
Genes outside of LADs (17,002)
Spearman's rho=0.98
All genes (19,469)
Fraction of genes with pS22-Lamin A/C-binding sites
Low
High
Gene decile by stratified by GRO-seq coverage
F
pS22-Lamin A/C-binding sites vs. transcription of genes stratified by gene length or gene-gene distance
Gene quartiles stratified by:
Gene length
Gene-to-gene distance
Short
Long
Fraction (%) of genes with pS22-Lamin A/C-binding sites
Number: Spearman's rho
Low
High
Gene decile stratified by GRO-seq coverage

Figure S3. Chromatin characteristics of pS22-Lamin A/C-binding sites (related to Figures 2 and 3)

(A) Fraction of the 22,966 pS22-Lamin A/C-binding sites that overlap ATAC-seq-defined accessible sites, H3K27ac ChIP-seq peaks, or H3K4me3 ChIP-seq peaks in BJ-5ta.

(B) ATAC-seq and ChIP-seq fold-enrichment (FE) scores at the 73,933 ATAC-seq-defined accessible sites in BJ-5ta.

(C) Fraction of pS22-Lamin A/C-bound or -unbound ATAC sites overlapping c-Jun-binding sites. ATAC sites (total 73,933 sites) are stratified into deciles by ATAC FE scores, and from each decile, 100 pS22-Lamin A/C-bound and 100 pS22-Lamin A/C-unbound ATAC sites are randomly selected, and the intersection is assessed. Fisher's exact test compares association between being bound by pS22-Lamin A/C and being bound by c-Jun, and P-values are adjusted by the Benjamini-Hochberg method.

(D) c-Jun and H3K27ac ChIP-seq FE scores at c-Jun-binding sites bound or unbound by pS22-Lamin A/C. c-Jun-binding sites (total 87,988 sites) are stratified into deciles by ATAC FE scores, and from each decile, 100 pS22-Lamin A/C-bound and 100 pS22-Lamin A/C-unbound ATAC sites are randomly selected, and their FE score distribution is visualized. Sum of FE scores within +/–250 bp of ATAC site center is used for analysis. Mann-Whitney *U*-test compares FE scores between pS22-Lamin A/C-bound and -unbound sites, and P-values are adjusted for multiple comparisons by the Benjamini-Hochberg method.

(E) Fraction of genes with pS22-Lamin A/C-binding sites (within gene body or 100 kb upstream) in gene decile stratified by GRO-seq coverage in BJ-5ta. Genes are first stratified by GRO-seq coverage and then grouped by their TSS positions with respect to Lamin A/C LADs (either overlapped or not). Data for all genes (shown in **Fig. 3H**) is shown again here for comparison. Horizontal dotted line, fraction of all genes with pS22-Lamin A/C-binding sites.

(F) Same as **(E)**, but genes are stratified (after GRO-seq stratification) by gene length (left) or distance to closest genes (right).

Figure S4

A

RNA-seq data sets used in this study

Data ID	Donor type	Cell line name	*LMNA* genotype	Donor age	Donor sex	GEO accession	Data source
KI429	Normal	GM08398	N/A	8 yrs	M	GSM3104038	This study
KI430	Normal	GM07492	N/A	17 yrs	M	GSM3104039	This study
KI433	Normal	GM08398	N/A	8 yrs	M	GSM3104042	This study
KI434	Normal	GM07492	N/A	17 yrs	M	GSM3104043	This study
s75	Normal	GM00969	N/A	2 yrs	F	GSM3124626	Fleischer et al.
s76	Normal	GM05565	N/A	3 yrs	M	GSM3124627	Fleischer et al.
s77	Normal	GM00498	N/A	3 yrs	M	GSM3124628	Fleischer et al.
s78	Normal	GM05381	N/A	5 yrs	M	GSM3124629	Fleischer et al.
s79	Normal	GM05400	N/A	6 yrs	M	GSM3124630	Fleischer et al.
s80	Normal	GM05757	N/A	7 yrs	M	GSM3124631	Fleischer et al.
s81	Normal	GM00409	N/A	7 yrs	M	GSM3124632	Fleischer et al.
s82	Normal	GM00499	N/A	8 yrs	M	GSM3124633	Fleischer et al.
s83	Normal	GM08398	N/A	8 yrs	M	GSM3124634	Fleischer et al.
s84	Normal	GM00038	N/A	9 yrs	F	GSM3124635	Fleischer et al.
KI431	HGPS	AG11498	1824C>T	14 yrs	M	GSM3104040	This study
KI432	HGPS	HGADFN167	1824C>T	8 yrs 5 mos	M	GSM3104041	This study
KI435	HGPS	AG11498	1824C>T	14 yrs	M	GSM3104044	This study
KI436	HGPS	HGADFN167	1824C>T	8 yrs 5 mos	M	GSM3104045	This study
s42	HGPS	AG11513	1824C>T	8 yrs	F	GSM3124693	Fleischer et al.
s43	HGPS	HGADFN167	1824C>T	8 yrs 5 mos	M	GSM3124694	Fleischer et al.
s44	HGPS	HGADFN188	1824C>T	2 yrs 3 mos	F	GSM3124695	Fleischer et al.
s45	HGPS	HGADFN127	1824C>T	3 yrs 9 mos	F	GSM3124696	Fleischer et al.
s46	HGPS	HGADFN164	1824C>T	4 yrs 8 mos	F	GSM3124697	Fleischer et al.
s47	HGPS	HGADFN169	1824C>T	8 yrs 6 mos	M	GSM3124698	Fleischer et al.
s48	HGPS	HGADFN178	1824C>T	6 yrs 11 mos	F	GSM3124699	Fleischer et al.
s49	HGPS	HGADFN122	1824C>T	5 yrs 0 mos	F	GSM3124700	Fleischer et al.
s50	HGPS	HGADFN143	1824C>T	8 yrs 10 mos	M	GSM3124701	Fleischer et al.
s51	HGPS	HGADFN367	1824C>T	3 yrs 0 mos	F	GSM3124702	Fleischer et al.

Normal, normal individual;
HGPS, patients with Hutchinson-Gilford Progeria Syndrome
N/A, not available; M, male; F, female
Fleischer et al, *Genome Biology* (2018) PMID: 30567591

B

Beta-galactosidase assay for senescence evaluation

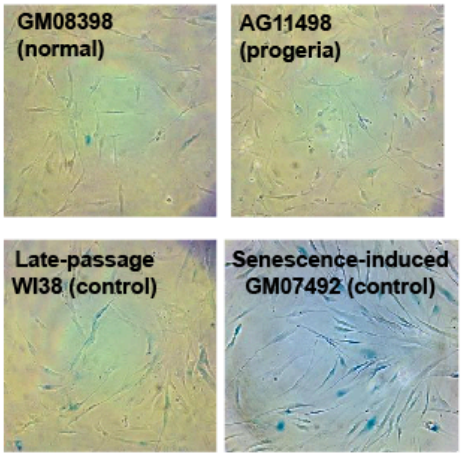

C

Quantification of beta-galactosidase assay

	Cell line	Condition	Positive cell %	Total cell count
Control	WI38	Early passage (PD25)	0%	206
	WI38	Late passage (PD41)	75%	156
	WI38	400 μM H_2O_2 (induced)	83%	151
	GM07	300 μM H_2O_2 (induced)	47%	201
Normal	GM07	Upon harvest	0.5%	195
	GM08	Upon harvest	2%	206
Progeria	AG11	Upon harvest	3%	206
	HG16	Upon harvest	1.5%	201

D

Principal component analysis of normal and progeria RNA-seq data sets with data ID annotation

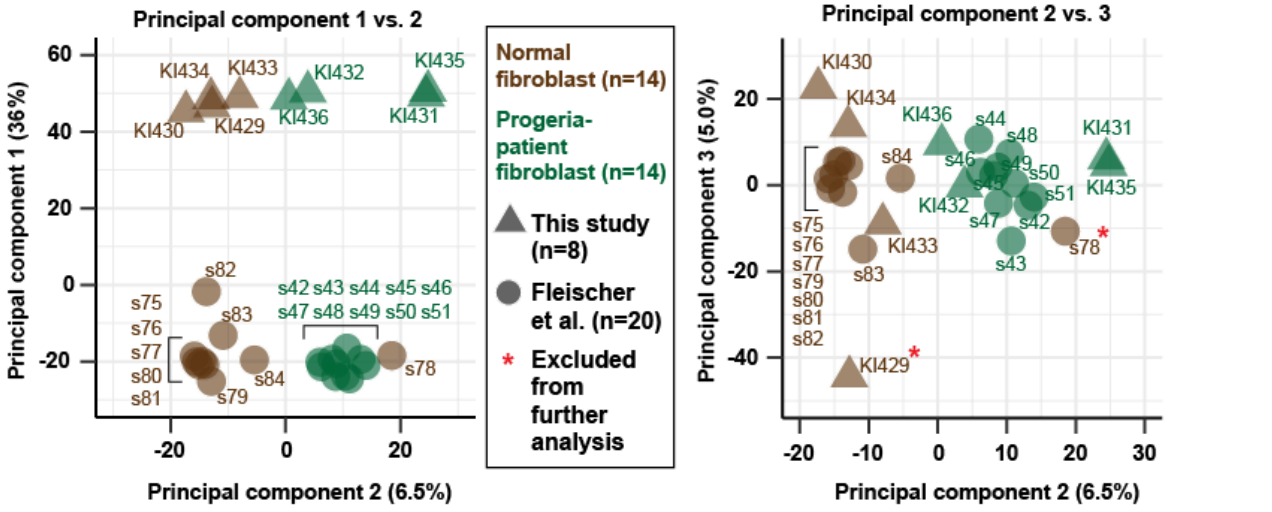

Figure S4. RNA-seq in progeria-patient and normal fibroblasts (related to Figure 4)

(A) The 28 RNA-seq datasets used in this study.

(B) Representative images of beta-galactosidase assay evaluating the extent of cell senescence. The assay was performed in the first biological replicate of cells used in RNA-seq and ChIP-seq.

(C) Quantification of beta-galactosidase assay. Early-passage WI38 fibroblasts serve as a negative control. Late-passage WI38 serves as a positive control. WI38 and GM07492 cells treated with H_2O_2 serve as additional positive controls. Cell line notation: GM08, GM08398. GM07, GM07492. AG11, AG11498. HG16, HGADFN167.

(D) Principal component analyses (PCA) of the 28 RNA-seq datasets with sample labels. PCA was performed on RNA-seq RPKMs for all 31,561 genes (see *Gene annotation* in **Methods**). The left panel without sample labels is shown in **Fig. 4A**.

Figure S5

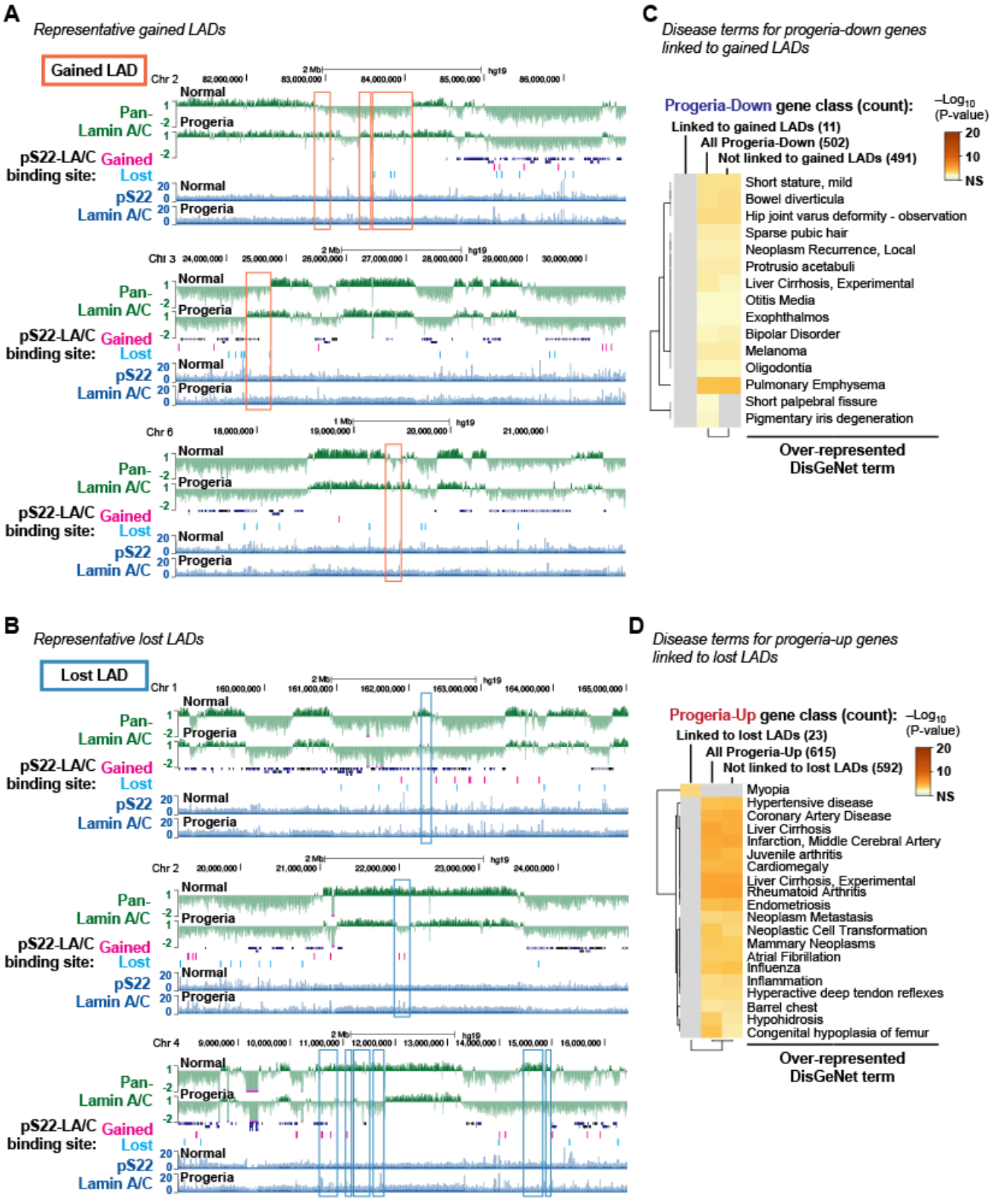
A
Representative gained LADs
Gained LAD
Chr 2
Chr 3
Chr 6
Normal
Progeria
Pan-Lamin A/C
pS22-LA/C binding site:
Gained
Lost
pS22
Lamin A/C
B
Representative lost LADs
Lost LAD
Chr 1
Chr 2
Chr 4
C
Disease terms for progeria-down genes linked to gained LADs
Progeria-Down gene class (count):
Linked to gained LADs (11)
All Progeria-Down (502)
Not linked to gained LADs (491)
−Log10 (P-value)
20
10
NS
Short stature, mild
Bowel diverticula
Hip joint varus deformity - observation
Sparse pubic hair
Neoplasm Recurrence, Local
Protrusio acetabuli
Liver Cirrhosis, Experimental
Otitis Media
Exophthalmos
Bipolar Disorder
Melanoma
Oligodontia
Pulmonary Emphysema
Short palpebral fissure
Pigmentary iris degeneration
Over-represented DisGeNet term
D
Disease terms for progeria-up genes linked to lost LADs
Progeria-Up gene class (count):
Linked to lost LADs (23)
All Progeria-Up (615)
Not linked to lost LADs (592)
Myopia
Hypertensive disease
Coronary Artery Disease
Liver Cirrhosis
Infarction, Middle Cerebral Artery
Juvenile arthritis
Cardiomegaly
Liver Cirrhosis, Experimental
Rheumatoid Arthritis
Endometriosis
Neoplasm Metastasis
Neoplastic Cell Transformation
Mammary Neoplasms
Atrial Fibrillation
Influenza
Inflammation
Hyperactive deep tendon reflexes
Barrel chest
Hypohidrosis
Congenital hypoplasia of femur
Over-represented DisGeNet term

Figure S5. Gained and lost LADs in progeria-patient fibroblasts (related to Figure 5)

(A) Representative pan-N-terminal-Lamin A/C (pan-Lamin A/C) and pS22-Lamin A/C ChIP-seq profiles in normal (GM07492) and progeria-patient (AG11498) fibroblasts. Signals are fold-enrichment (FE) scores. Box, gained LADs in progeria-patient fibroblasts. Pan-N-terminal-Lamin A/C profiles are in the $\log_2$ scale to visualize LAD patterns.

(B) Same as **(A)**, but boxes indicate lost LADs in progeria-patient fibroblasts.

(C) DisGeNet-curated disease terms over-represented among progeria-down genes linked to gained LADs, progeria-down genes not linked to gained LADs, and all progeria-down genes. No terms are enriched among progeria-down genes linked to gained LADs.

(D) Same as **(C)**, but progeria-up genes linked to lost LADs, progeria-up genes not linked to lost LADs, and all progeria-up genes are shown.

Figure S6

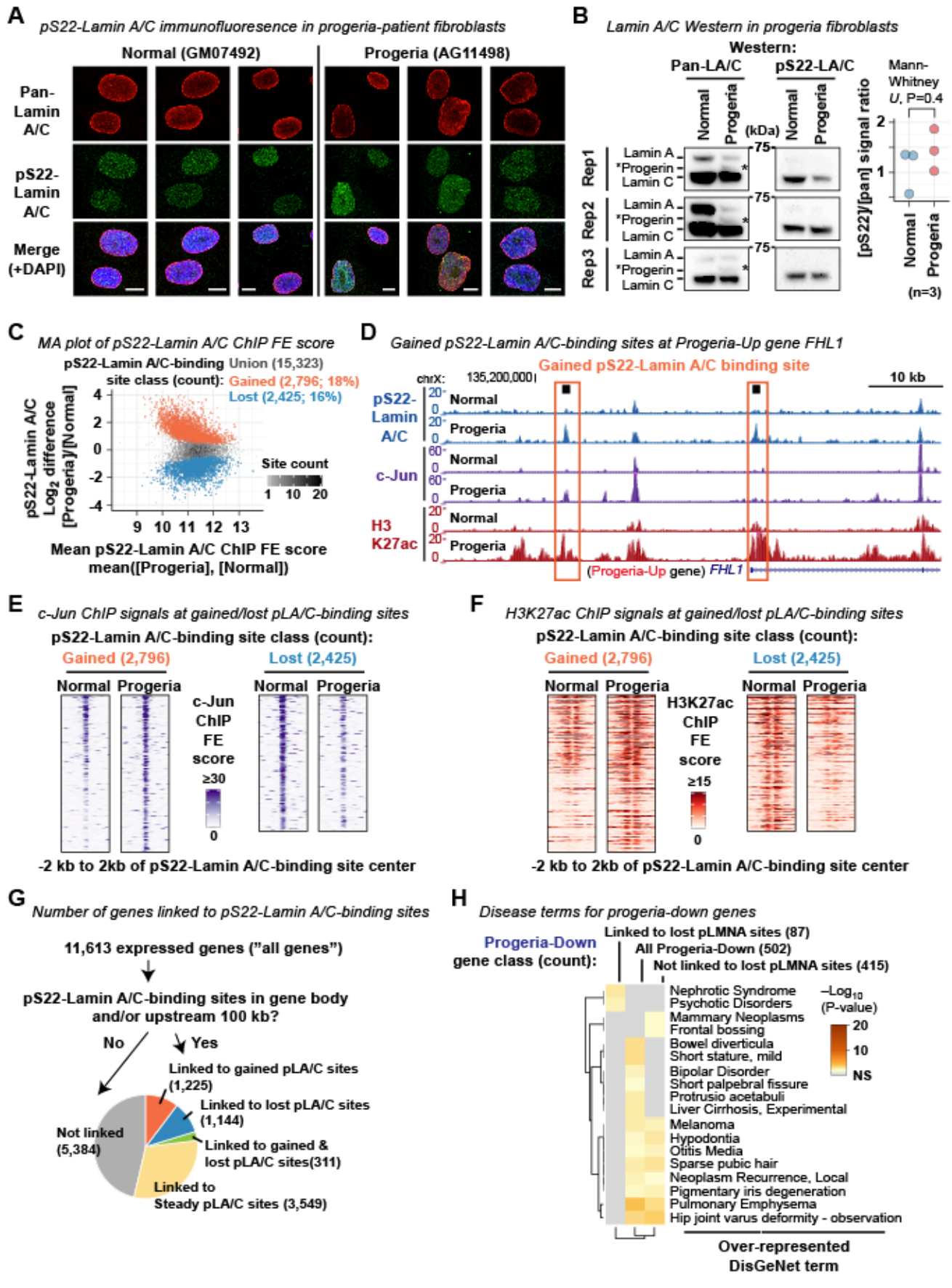
A
pS22-Lamin A/C immunofluoresence in progeria-patient fibroblasts
Normal (GM07492)
Progeria (AG11498)
Pan-Lamin A/C
pS22-Lamin A/C
Merge (+DAPI)
B
Lamin A/C Western in progeria fibroblasts
Western:
Pan-LA/C
pS22-LA/C
Normal
Progeria
(kDa)
Rep1
Rep2
Rep3
Lamin A
*Progerin
Lamin C
75
Mann-Whitney U, P=0.4
[pS22]/[pan] signal ratio
(n=3)
C
MA plot of pS22-Lamin A/C ChIP FE score
pS22-Lamin A/C-binding site class (count):
Union (15,323)
Gained (2,796; 18%)
Lost (2,425; 16%)
pS22-Lamin A/C Log2 difference [Progeria]/[Normal]
Site count
Mean pS22-Lamin A/C ChIP FE score mean([Progeria], [Normal])
D
Gained pS22-Lamin A/C-binding sites at Progeria-Up gene FHL1
Gained pS22-Lamin A/C binding site
chrX:
135,200,000
10 kb
pS22-Lamin A/C
c-Jun
H3 K27ac
Normal
Progeria
(Progeria-Up gene) FHL1
E
c-Jun ChIP signals at gained/lost pLA/C-binding sites
pS22-Lamin A/C-binding site class (count):
Gained (2,796)
Lost (2,425)
c-Jun ChIP FE score
≥30
-2 kb to 2kb of pS22-Lamin A/C-binding site center
F
H3K27ac ChIP signals at gained/lost pLA/C-binding sites
pS22-Lamin A/C-binding site class (count):
Gained (2,796)
Lost (2,425)
H3K27ac ChIP FE score
≥15
-2 kb to 2kb of pS22-Lamin A/C-binding site center
G
Number of genes linked to pS22-Lamin A/C-binding sites
11,613 expressed genes ("all genes")
pS22-Lamin A/C-binding sites in gene body and/or upstream 100 kb?
No
Yes
Linked to gained pLA/C sites (1,225)
Linked to lost pLA/C sites (1,144)
Linked to gained & lost pLA/C sites(311)
Linked to Steady pLA/C sites (3,549)
Not linked (5,384)
H
Disease terms for progeria-down genes
Progeria-Down gene class (count):
Linked to lost pLMNA sites (87)
All Progeria-Down (502)
Not linked to lost pLMNA sites (415)
Nephrotic Syndrome
Psychotic Disorders
Mammary Neoplasms
Frontal bossing
Bowel diverticula
Short stature, mild
Bipolar Disorder
Short palpebral fissure
Protrusio acetabuli
Liver Cirrhosis, Experimental
Melanoma
Hypodontia
Otitis Media
Sparse pubic hair
Neoplasm Recurrence, Local
Pigmentary iris degeneration
Pulmonary Emphysema
Hip joint varus deformity - observation
−Log10 (P-value)
NS
Over-represented DisGeNet term

Figure S6. Gained and lost pS22-Lamin A/C-binding sites in progeria-patient fibroblasts (related to Figure 6)

(A) Immunofluorescence using the anti-pan-N-terminal Lamin A/C antibody and anti-pS22-Lamin A/C antibody in normal and progeria fibroblasts. Representative images from 3 biological replicates are shown.

(B) (Left) Western blot for pan-N-terminal-Lamin A/C and pS22-Lamin A/C on normal (GM07492) and progeria fibroblast (AG11498) extracts. Asterisks indicate the Western blot signals for progerin.

(C) MA plot for the 15,323 union pS22-Lamin A/C-binding sites, highlighting gained and lost pS22-Lamin A/C-binding sites. Sum of pS22-Lamin A/C ChIP FE scores within +/–250 bp of the site center is compared. Normal, normal fibroblast GM07492. Progeria, progeria fibroblast AG11498.

(D) pS22-Lamin A/C, c-Jun, and H3K27ac ChIP-seq profiles at the *FHL-1* locus highlighting gained pS22-Lamin A/C-binding sites. Signals are FE scores. The *FHL-1* gene is among the genes up-regulated in progeria fibroblasts, and its mutations cause cardiac and skeletal myopathies. Normal, GM07492 normal fibroblast. Progeria, AG11498 progeria fibroblast.

(E) c-Jun ChIP-seq FE score distribution around gained pS22-Lamin A/C-binding sites and lost pS22-Lamin A/C-binding sites.

(F) Same as **(E)** but H3K27ac ChIP-seq FE scores are shown.

(G) Number and fraction of genes linked to gained, lost, and steady pS22-Lamin A/C-binding sites.

(H) DisGeNet-curated disease terms over-represented among progeria-down genes linked to lost pS22-Lamin A/C-binding sites, or those not linked to lost pS22-Lamin A/C-binding sites, or all progeria-down genes.